Neutron scattering and thermal studies of the Ni-incorporated CeSbNi$_x$ system

D. T. Adroja,[1,2] J. G. M. Armitage,[2] P. C. Riedi,[2] M. H. Jung,[3] Z. Tun,[4] and T. Takabatake[3]

[1]*ISIS Facility, Rutherford Appleton Laboratory, Chilton, Didcot, Oxon OX11 0QX, United Kingdom*
[2]*School of Physics and Astronomy, St. Andrews University, St. Andrews KY16 9SS, United Kingdom*
[3]*Department of Quantum Matters, ADSM, Hiroshima University, Higashi-Hiroshima 739-8526, Japan*
[4]*NPMR, NRC, AECL, Chalk River Laboratories, Chalk River, Ontario, Canada K0J 1J0*

Neutron scattering, thermal expansion, and magnetostriction measurements have been carried out on the cubic compounds CeSbNi$_x$ ($x=0-0.4$). Inelastic neutron scattering studies show a well-defined crystal field (CF) excitation at 4.06 (±0.04) meV and 5.02(±0.05) meV in $x=0.08$ and 0.15, respectively. The crystal field splitting increases with x compared with the parent compound CeSb (3.19 meV) in spite of the lattice parameter increasing with Ni incorporation. The implication is that the increase in the CF splitting in $x=0.08$ and 0.15 is due to a collapse of the p-f mixing between the Sb $5p$ holes and the localized Ce $4f$ electrons. The analysis of inelastic spectra of $x=0.15$ shows that the ground state is a doublet (Γ_7), which explains the temperature-dependent behavior of the magnetic susceptibility. Thermal expansion shows a dramatic change in behavior with Ni composition. The thermal expansion coefficient exhibits a first-order transition at 15.4 K in CeSb, which disappears for Ni composition as low as $x=0.035$, as well as in an applied field of 8 T. A large magnetostriction has been observed in CeSb in the magnetic-ordered state as well as in the paramagnetic state. The absolute values of the magnetostriction are reduced considerably in the Ni-incorporated alloys. The volume magnetostriction of $x=0.15$ alloy exhibits a scaling behavior in the paramagnetic state from which we have estimated the product of the magnetovolume coupling constant and the isothermal compressibility.

I. INTRODUCTION

A number of interesting magnetic and transport properties have been reported in the Ce-monopnictides compounds CeX ($X=$P, As, Sb, and Bi) which crystallize in the simple rock-salt, NaCl-type, structure.[1] In the NaCl-type structure of these compounds, the Ce site has octahedral symmetry, which splits the $J=5/2$ ground-state multiplet in to a doublet (Γ_7) and a quartet (Γ_8). For all these compounds the crystal field ground state is a doublet Γ_7.[2–6] In the CeX series the crystal field splitting (Δ_{CF}) decreases with increasing size of anion atom (i.e., with increasing cubic lattice parameter a), while the Néel temperature (T_N) increases with the size of anion atom: $\Delta_{CF}=14.82$ MeV (at 15 K), 13.70 MeV (at 12 K), 3.19 MeV (at 20 K), and 0.69 meV (at 120 K), and $a=5.93$, 6.08, 6.41, and 6.50 Å (at 300 K), and $T_N=8.5$, 7.5, 16.1, and 25.2 K for $X=$P, As, Sb, and Bi, respectively.[3] From the inelastic neutron scattering studies of CeSb at 300 K, the upper limit of the crystal field (CF) splitting was put to 2.15 meV.[2] The compounds with $X=$P and As show a large CF splitting and a small T_N, while those with $X=$Sb and Bi show a small CF splitting and a large T_N. This shows that the crystal field interaction dominates in the former, while the magnetic exchange interaction is dominant in the latter. The crystal field splitting 3.19 meV (0.69 meV) of CeSb (CeBi) is unusually small compared with the 22.75 meV (21.28 meV) expected from the extrapolation from the other members of the rare-earth compounds in this series.[6] This small value of CF splitting has been explained on the basis of the p-f mixing model.[7–10] In this model the ground-state crystal field level Γ_7 has very small mixing with the predominant Ce $5d$ conduction band, but the excited CF level Γ_8 has strong mixing with the holes of the valence band of Sb $5p$, and hence the strong p-f mixing effect is expected for a larger number of holes. The latter mechanism pushes the Γ_8 level away from the Fermi level and hence reduces the CF splitting between Γ_7 and Γ_8 compared with that predicted by the point charge model.

The compound CeSb is well known for its complex magnetic phase diagram and strongly anisotropic magnetic properties below T_N.[11,12] Unusual and complex magnetic properties come from the p-f (Γ_8) mixing, while the transport properties are due to d-f (Γ_7) mixing. The various magnetic structures are formed by a periodic stacking of ferromagnetic (001) planes, with magnetic moments pointing up or down, and paramagnetic planes. The coexistence of the ferromagnetic and paramagnetic planes is due to a delicate balance between the small crystal field splitting and the number of holes in the valence band. The easy magnetization axis is along the $\langle 001 \rangle$ direction, in contrast to the $\langle 111 \rangle$ easy axis predicted by the crystal field only. The magnetic ordering is accompanied by a large structural distortion from cubic to tetragonal.[13] The zero-field specific heat exhibits seven phase transitions between 17 and 8 K, while the specific heat in an applied field reveals the presence of nonmagnetic planes in some magnetic phases.[14] The P-T phase diagram of CeSb also exhibits interesting behavior, which shows the existence of a critical end point at a pressure of 2 kbar and 18 K at which a line of critical points corresponding to the second-order phase transition ends on a line of the first-order phase transition.[12]

Recently, we have found that Ni atoms can be incorporated in the cubic CeSb, which increases the lattice parameter almost linearly with Ni composition at a rate of $da/dx=0.0849$ Å.[15] Our study revealed that up to 40% (i.e., x

=0.4) of Ni, the material crystalizes in a single-phase cubic structure. The Ni atoms occupy interstitial sites in CeSb, which change the magnetic and transport properties dramatically. This dramatic change in the magnetic property has been attributed to the considerable reduction in the *p-f* mixing,[15] while the change in the transport property is due to the increase of the *d*-electron concentration, which increases the *d-f* mixing. A recent study by neutron diffraction using a four-circle diffractometer on a CeSbNi$_{0.15}$ single crystal showed that the Ni atom occupies the (1/4, 1/4, 1/4) site in the NaCl-type structure.[16] In order to gain further information about the crystal field splitting, magnetic structure, and thermodynamical properties, such as the thermal expansion and magnetostriction, we have carried out neutron scattering, thermal expansion, and magnetostriction measurements on CeSbNi$_x$ ($x=0-0.4$) alloys. The results of these studies are presented in this paper. The layout of the paper is as follows. In Sec. II we outline the experimental techniques used in the present work. The results of inelastic neutron scattering experiments on $x=0.08$ and 0.15 alloys are presented in Sec. III A. A brief discussion of the magnetic structure of $x=0.15$ alloy is given in Sec. III B. The analysis of the magnetic susceptibility results for a single crystal of CeSbNi$_{0.15}$ on the basis of a crystal field model is given in Sec. III C. In Sec. III D we present our thermal expansion results on CeSbNi$_x$ ($x=0$, 0.035, 0.15, and 0.4) and give a comparison with the previous study on CeSb. The results of magnetostriction measurements on $x=0$, 0.15, and 0.4 are discussed in Sec. III E. The main conclusions of the present work are given in the final section.

II. EXPERIMENTAL DETAILS

The polycrystalline samples of CeSbNi$_x$ ($x=0, 0.035, 0.08, 0.15, 0.4$) were prepared by the arc melting technique as described in Ref. 15. The single crystal of CeSbNi$_{0.15}$ was grown by the Bridgman method in a Mo crucible. The phase purity of the samples was checked using the x-ray powder diffraction technique, which showed that the materials were nearly single phase and crystallize in the cubic structure. The thermal expansion and magnetostriction samples, $x=0$, 0.15, and 0.4, are the same as those on which magnetic susceptibility and resistivity studies have been reported.[15] The inelastic neutron scattering measurements were carried out using the C5 triple-axis spectrometer at NRU reactor, Chalk River Laboratory, Canada. The spectrometer was operated in the fixed final energy ($E_f = 14.56$ meV) mode. We used pyrolytic graphite [PG(002)] crystals for both monochromator and analyzer. To reduced higher-order contamination a pyrolytic graphite filter was placed between the sample and analyzer. The collimations used in the present experimental setting of the spectrometer were open-48′-56′-open. This configuration gave us a maximum energy transfer of 8 meV with a typical energy resolution of 0.9 meV [full width at half maximum (FWHM)] at the elastic position. A standard ^{4}He cryostat (a closed-cycle refrigerator for $x=0.08$) was used for the low-temperature measurements. The polycrystalline sample of weight about 18 g was sealed in a thin-wall aluminum can (vanadium can for $x=0.08$) of 15 mm diameter and 62 mm length. The magnetic origin of the observed excitation was confirmed
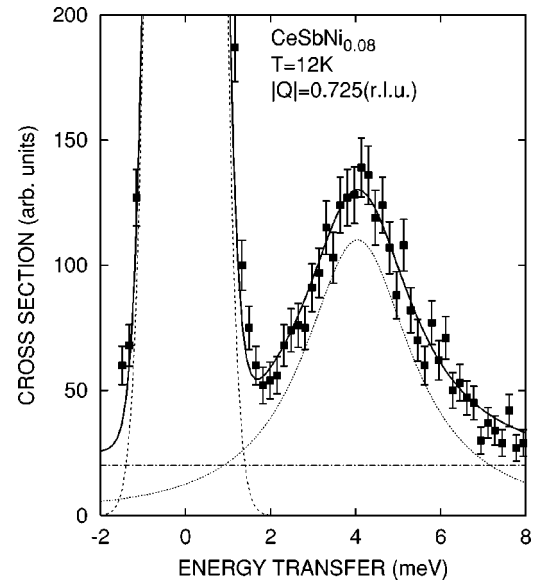

FIG. 1. Inelastic neutron scattering response from polycrystalline CeSbNi$_{0.08}$ in the paramagnetic state at 12 K for $|Q|=0.725$ (r.l.u.). The solid line represents the fit, whereas the dotted lines are the components of the fitted function (see text).

from the measurements carried out at a larger value of Q and also at different temperatures. The magnetic susceptibility of the CeSbNi$_{0.15}$ single crystal was measured using a superconducting quantum interference device (SQUID) magnetometer between 2 and 300 K in an applied field of 0.5 T. Thermal expansion and magnetostriction measurements were carried out in a parallel plate capacitance cell that had been calibrated using the known thermal expansivity of Si. The disk-shaped samples with diameter 4.5 mm and thickness 1.5–2 mm were cut using a spark cutting machine for the thermal expansion and magnetostriction measurements. A magnetic field up to 8 T was applied in the plane of the disk using a superconducting magnet. The relative accuracy of the method was $\Delta L/L \approx 1 \times 10^{-7}$.

III. RESULTS AND DISCUSSION

A. Inelastic neutron scattering

Figures 1 and 2 show the measured inelastic (INS) response from CeSbNi$_x$ ($x=0.08$ and 0.15 with the cubic lattice parameters $a=6.427$ and 6.438 Å, respectively) at low temperatures. At a low value of $|Q|=0.725$ (r.l.u.) and at 12 K, the inelastic response shows a well-defined excitation centered at 4.06($\pm$0.04) meV with a linewidth of 2.66 ($\pm$0.04) meV for the 8% alloys and 5.02($\pm$0.05) meV with a linewidth 3.38($\pm$0.02) meV for the 15% alloy. The quasielastic response is also observed centered at zero-energy transfer in both the alloys. The intensity of the inelastic peak decreases with either increasing $|Q|$ or temperature (50 K; see Fig. 2). The Q dependence of the peak intensity follows $F(Q)^2$ behavior, where $F(Q)$ is the Ce^{3+} magnetic form factor as calculated in the dipole approximation.[17] On the other hand, the temperature-dependent intensity of the peak shows the behavior predicted by Boltzmann statistics. We therefore conclude that the peak is of magnetic origin and the nonmagnetic scattering contribution such as phonon scatter-
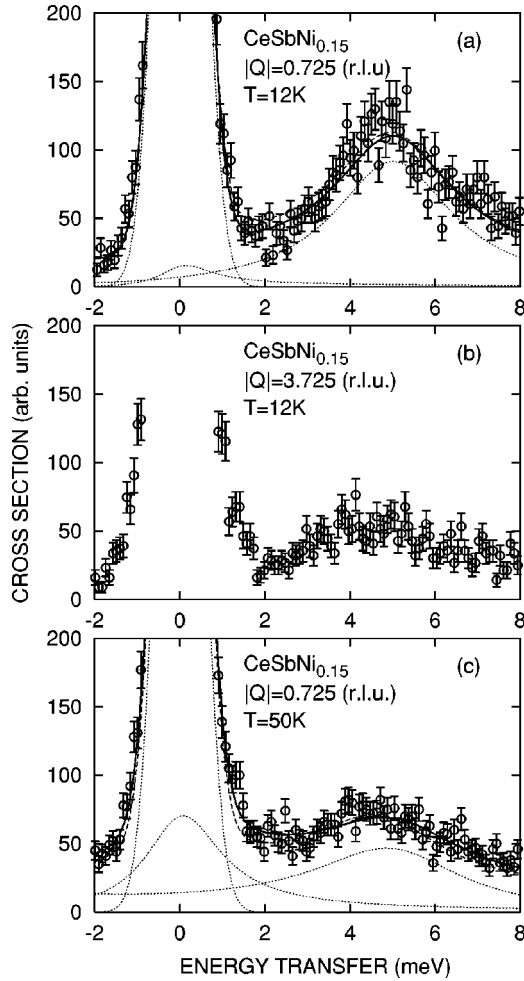
FIG. 2. Inelastic neutron scattering response from polycrystalline $CeSbNi_{0.15}$ in the paramagnetic state (a) at 12 K, $|Q|=0.725$ (r.l.u.), (b) at 12 K, $|Q|=3.725$ (r.l.u.), and (c) at 50 K, $|Q| = 0.725$ (r.l.u.). The solid lines represent the result of the least-squares fit to a quasielastic and inelastic Lorentzian as described in the text (dotted lines represents the components of the fit). The dashed line (passing through the data points) represents a fit based on the crystal field model with Γ_7 as a ground state (see text).

ing is negligible in the measured temperature and energy range. The peak in the inelastic response is due to the crystal field transition from the ground-state CF level to the excited CF level of the Ce^{3+} ions. The observed CF splitting in $CeSbNi_x$ ($x=0.08$ and 0.15) alloys is higher than that in CeSb [3.19 meV (Refs. 2–4)] even though the lattice parameter increases with x.[15] On the basis of a simple point charge model, one would expect the CF splitting to decrease with increasing cubic lattice parameter a as $\Delta_{CF} \propto 1/a^5$.[3,6] Further, the inelastic spectra of $CeSbNi_{0.15}$ at 4.2 K also exhibit an inelastic peak centered at 4.89($\pm$0.05) meV, with a linewidth of 3.48($\pm$0.03) meV: no clear sign of the splitting of the inelastic peak due to the molecular field was observed. In addition to the 4.89 meV peak, we also observed a weak response near zero-energy transfer, which could be fitted better with an inelastic peak centered at 1.15($\pm$0.02) meV than the quasielastic peak. However, our instrument resolution was not sufficient to resolve clearly this excitation from the elastic scattering.

The point symmetry of Ce ions in $CeSbNi_X$ is cubic, which gives only one independent CF parameter in the CF Hamiltonian, $H_{CF} = B_4^0(O_4^0 + 5O_4^4)$, where B_4^0 is the crystal field parameter and O_m^n are the Stevens operators.[18] Under the cubic CF potential the $J=5/2$ multiplet of the Ce^{3+} ions splits into a doublet (Γ_7) and a quartet (Γ_8), with energy eigenvalues of $-240B_4^0$ and $120B_4^0$, respectively.[19] This gives a direct method of estimating the CF parameter from the measured position of the inelastic excitation, $\Delta_{CF} = 360B_4^0$.[19] However, from the peak position only it is not possible to determine the sign of B_4^0, i.e., to decide whether the CF ground state is a doublet Γ_7 or a quarter Γ_8. In order to determine the ground state, one needs to compare the observed intensities of the quasielastic and inelastic peaks and also their temperature dependences with those calculated on the basis of CF model.[20] At low temperatures the contribution to the quasielastic scattering comes from the scattering of the electrons within the ground-state CF level, but at high temperatures, when the excited state is populated, scattering within the excited state also contributes to the quasielastic scattering.

To determine the ground state of the Ce^{3+} ion in $CeSbNi_{0.15}$, the inelastic response was fitted to a sum of a quasielastic Lorentzian line centered at zero-energy transfer and an inelastic symmetric Lorentzian line centered at $\pm\Delta_{CF}$, where Δ_{CF} is the CF splitting. The quasielastic contribution was fitted by convoluting the instrument resolution function, which is a Gaussian function. The instrument resolution was estimated from measurements of a vanadium sample under identical conditions. However, in the case of $x=0.08$ alloy due to the presence of strong incoherent scattering from the vanadium can and weak quasielastic scattering from the sample, it was not possible to fit the quasielastic peak accurately. Hence spectra of $x=0.08$ were fitted to only one inelastic peak along with the elastic response. The solid lines in Figs. 1 and 2 show the best fit to the data by the least-squares fitting procedure. The components of the fit are shown by dotted lines in Figs. 1 and 2. The estimated linewidth of the quasielastic and inelastic peaks for $x=0.15$ are 1.46($\pm$0.35) meV and 3.38($\pm$0.2) meV at 12 K and 2.16($\pm$0.70) meV and 4.24($\pm$0.49) meV at 50 K, respectively. The position of the inelastic line at 12 K(5.02 ± 0.05 meV) and 50 K(5.11 ± 0.11 meV), indicates the temperature independence of the crystal field within experimental accuracy. This is also the case in CeSb, while strong temperature-dependent CF splitting has been observed for CeP and CeAs.[3] Further, the width of the inelastic peak at 12 K is slightly higher than 2.4 ± 0.4 meV observed in CeSb at 20 K.[3] The intensity of the quasielastic peak increases with temperature, while that of the inelastic peak decreases with increasing temperature. The intensity ratio of the quasielastic peaks at 12 and 50 K is 0.51, which is close to the calculated value of 0.63 for a doublet ground state (for a quartet ground state, the calculated ratio is 1.08). Further, the observed ratio for the inelastic peak at 12 and 50 K is 2.3, which is close to the calculated ratio of 1.6 for a doublet ground state (for a quartet ground state, the calculated ratio is 1.16). This indicates that the ground state of $CeSbNi_{0.15}$ is a doublet.

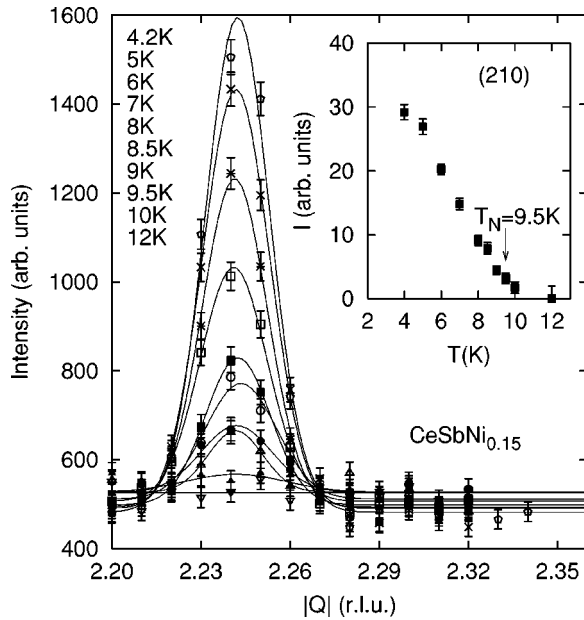To further check the proposed energy-level scheme, we have analyzed the low $|Q|=0.725$ r.l. inelastic spectra at 12

FIG. 3. Elastic Q scans of CeSbNi$_{0.15}$ at various temperatures. The solid lines represent the fits to a Gaussian function. The inset shows the integrated intensity of the (210) peak at various temperatures.

and 50 K by solving the cubic crystal field Hamiltonian and least-squares fitting the neutron scattering cross section to the experimental data. The fits were made taking the ground state as a doublet as well as a quartet. A better fit to the data at 12 K was obtained for the doublet ground state than the quartet ground state. However, for the 50 K spectra the doublet and quartet ground states gave almost a similar fit. These results support the doublet ground state in CeSbNi$_{0.15}$.

B. Elastic neutron scattering

To obtain information about the magnetic structure of CeSbNi$_{0.15}$, we have performed various elastic Q scans using the triple-axis spectrometer at low temperatures. We found Bragg peaks at $|Q| = 2.24$ and 3.74 (r.l.u.), corresponding to a (210) and (321) reflections, respectively. These reflections were not observed at 12 K (i.e., above T_N). This shows that (210) and (321) reflections are magnetic in origin. The (210) reflection arises from $(220)_{\text{nuclear}} \pm (010)_{\text{magnetic}}$, while (321) arises from $(311)_{\text{nuclear}} \pm (010)_{\text{magnetic}}$. This reveals the antiferromagnetic structure of CeSbNi$_{0.15}$ is type I with $k = (010)(\uparrow\downarrow)$. The type-I antiferromagnetic structure was also observed in CeBi (between 25 and 12 K), CeSb$_{0.95}$Te$_{0.05}$, and CeSb$_{0.8}$As$_{0.2}$.[21] In order to check that the magnetic structure of CeSbNi$_{0.15}$ remains the same between T_N and 4.2 K, we measured the (210) reflection at various temperatures between 4.2 and 12 K (see Fig. 3). The peak intensity increases almost linearly between 10 and 5 K and shows a tendency to saturate below 5 K (inset to Fig. 3), which indicates that the magnetic structure remains the same between T_N and 4.2 K. The type-I antiferromagnetic magnetic structure observed in our polycrystalline sample of CeSbNi$_{0.15}$ between 4 and 12 K agrees well with the recent neutron diffraction studies carried out on a single crystal of CeSbNi$_{0.15}$.[16]

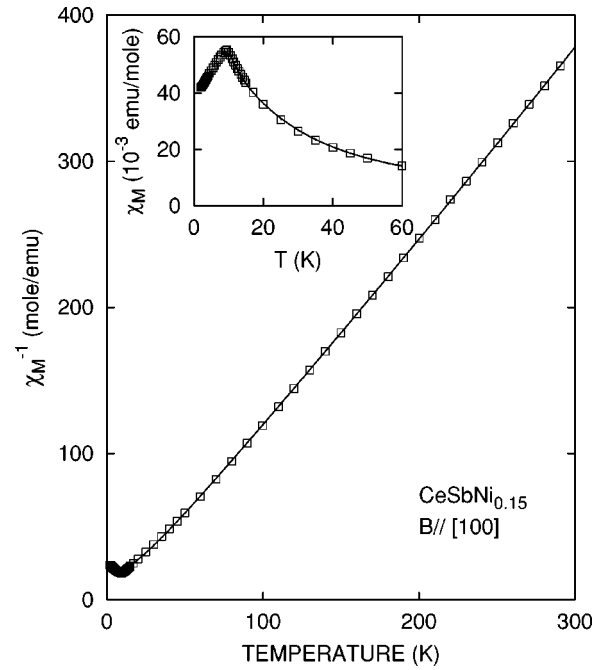FIG. 4. Inverse magnetic susceptibility vs temperature for CeSbNi$_{0.15}$ single crystal in an applied field of 0.5 T for **B**//[100]. The inset shows low-temperature behavior of the susceptibility for **B**//[100]. The solid line represents the fit based on the crystal field model (see text).

Recently, the complex magnetic phase diagram of CeSb has been explained by considering the interband exchange interaction in addition to the intraband exchange interaction.[22] The intraband exchange interaction (which is the usual Kondo exchange) induces a ferromagnetic coupling between the 4f moments due to the very low carrier concentration, whereas the interband interaction (which is spin-dependent exchange) favors an antiferromagnetic correlation. Therefore, the competition between the two interactions gives various types of magnetic structures in the phase diagram of CeSb.[22] The stability of the type-I antiferromagnetic phase in CeSbNi$_{0.15}$ suggests that intraband exchange has reduced considerably compared to interband exchange. The incorporation of Ni in CeSb fills the Sb5p holes that mix strongly with the excited crystal field level Γ_8 of Ce^{3+} ions due to the same symmetry. The reduction of the 5p-hole concentration should weaken both the intraband and interband exchange interactions. The intraband exchange is proportional to the square of the p-f mixing interaction, while the interband exchange is proportional to the product of the p-f mixing and the d-f mixing. The d-f mixing is independent of the Sb-5p-hole concentration, but increases with d-electron concentration. Therefore, as the p-f mixing is reduced with Ni incorporation, the intraband ferromagnetic interaction is weakened more than the interband antiferromagnetic interactions, which stabilizes the type-I antiferromagnetic ground state.

C. Magnetic susceptibility

The magnetic susceptibility of a CeSbNi$_{0.15}$ single crystal was measured between 2 and 300 K (Fig. 4) for the **B**∥[100] direction. The susceptibility exhibits Curie-Weiss (CW) be-

havior between 300 and 60 K and deviates from it below 60 K. The deviation from CW behavior is attributed to the effect of the crystal field on the $J=5/2$ state on Ce^{3+} ions. The values of effective magnetic moment (μ_{eff}) and paramagnetic Cure temperature (θ_P) obtained from the high-temperature CW behavior are $\mu_{eff}=2.54\mu_B$ and $\theta_P=6.1$ K, respectively. These values are comparable with $\mu_{eff}=2.56-2.58\mu_B$ and $\theta_P=5-8$ K for CeSb.[11,23] The observed value of μ_{eff} is the same compared with the value $2.54\mu_B$ expected for the Ce^{3+} ion with the $J=5/2$, which indicates that the nickel atoms do not carry magnetic moments. The observed positive sign of θ_P for CeSbNi$_{0.15}$ and CeSb suggests ferromagnetic-type correlations between the Ce moments at high temperatures, which is unusual for an antiferromagnetic ground state. Further, our low-temperature (below 20 K) susceptibility measurements for the $\mathbf{B}\|[110]$ direction show almost identical behavior to that of the $\mathbf{B}\|[100]$ direction.[15] This indicates that the magnetic properties of CeSbNi$_{0.15}$ are isotropic compared to the highly anisotropic magnetic properties observed in the parent CeSb below $T_N=16.5$ K.[11,23] The absence of magnetic anisotropy in CeSbNi$_{0.15}$ suggests that the strong anisotropic p-f mixing which is present in CeSb has reduced considerably. The temperature dependence of the susceptibility of CeSbNi$_{0.15}$ has been analyzed on the basis of the CF model, taking the ground state as a doublet:[24]

$$\chi(T)=\chi_{CF}(T)/[1-\lambda\chi_{CF}(T)]+\chi_0, \qquad (1)$$

where χ_{CF} is the paramagnetic susceptibility of the Ce^{3+} ion in the presence of the cubic crystal field, λ is a molecular field constant, and χ_0 is the temperature-independent contribution to the susceptibility arising from conduction electrons and core electrons. $\chi_{CF}(T)$ was calculated from the crystal field parameters obtained from the inelastic neutron scattering data at 12 K. The values of λ and χ_0 obtained from the least-squares fit were 6.25 and -0.00011 emu/mol, respectively. The solid line in Fig. 4 represents the fit which agrees well with the observed data. This shows that the susceptibility analysis also confirms that the CF ground state is a doublet in CeSbNi$_{0.15}$.

D. Thermal expansion

Figures 5(a)–5(c) show the linear thermal expansion ($\Delta L/L$) as a function of temperature for CeSbNi$_X$ ($x=0$, 0.035, 0.15, and 0.4) alloys along with the isostructural nonmagnetic reference compound LaSbNi$_{0.15}$. Note that the reference length was taken at 90 K. The $\Delta L/L$ of LaSbNi$_{0.15}$ gradually decreases with decreasing temperature from 90 K and becomes almost temperature independent below 20 K. This is a typical behavior expected from the thermally excited phonons. For CeSb (i.e., $x=0$), $\Delta L/L$ decreases with decreasing temperature from 90 K, exhibits a minimum around 45 K, and eventually drops sharply below 16.5 K due to the antiferromagnetic ordering of the Ce moments: a second transition in $\Delta L/L$ is observed around 14.8 K. The thermal expansion behavior is similar to that observed in a CeSb single-crystal sample.[25] The relative change of the length of the polycrystalline CeSb between T_N and 3 K is 9.2×10^{-4}, which is slightly smaller than the reported value (0.00129) for the single-crystal CeSb.[25] The change in the
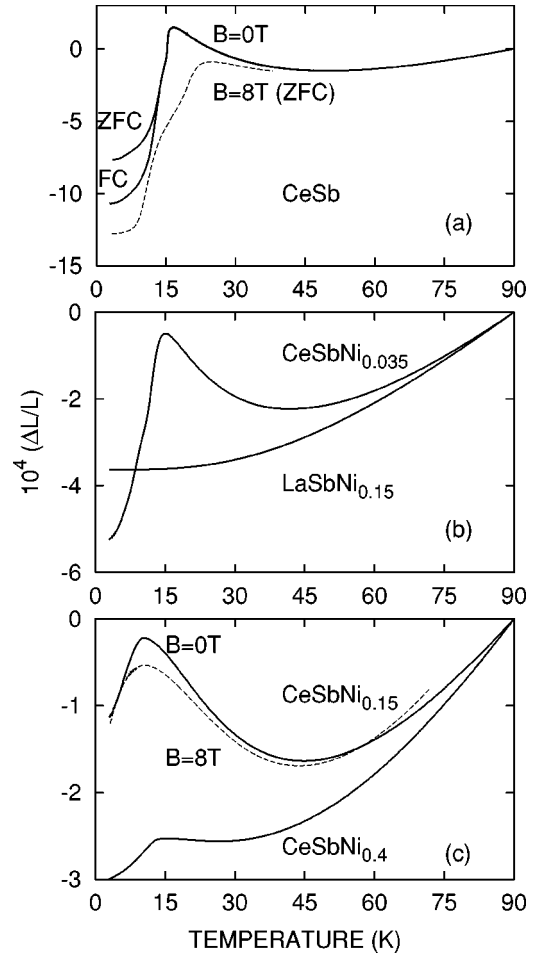

FIG. 5. Thermal expansion $\Delta L/L$ vs temperature for CeSbNi$_X$ ($x=0$, 0.035, 0.15, and 0.4) alloys. The magnetic field was applied parallel to $\Delta L/L$.

lattice parameters [$\Delta a/a(6$ K$)=0.00064$] has also been observed between T_N and 6 K from neutron diffraction studies on a single-crystal sample.[26] The sudden change in the length of CeSb below T_N has been shown to be due to the tetragonal distortion of the cubic unit cell arising from the presence of a strong magnetoelastic coupling.[17] With increasing Ni composition in CeSb, the observed minimum in the length becomes less pronounced and eventually almost disappears for $x=0.4$. Further, the change of the length below T_N also becomes smaller with increasing Ni composition, x. The observed first-order phase transition in the parent compound CeSb disappears for a Ni composition as low as $x=0.035$. This behavior reflects the sharp change in the magnetic structure with Ni incorporation. Almost similar behavior for thermal expansion has been reported in Ce$_{1-x}$La$_x$Sb ($x=0.2-0.5$) alloys:[25] the observed sharp drop at 16.5 K in $\Delta L/L$ of CeSb disappears, and the minimum at 45 K becomes less pronounced with La substitution.

To investigate the effect of a magnetic field, we have measured the thermal expansion in an applied field ($\mathbf{B}\|\Delta L/L$) of 8 T for $x=0$ and 0.15 alloys. The $\Delta L/L$ measured in the 8 T field (samples were cooled in zero field) shows a dramatic effect near T_N. For CeSb the temperature (16.5 K) at which $\Delta L/L$ exhibits a sharp drop in zero field increases to 22 K in the 8 T field and the second transition

temperature shifts to lower temperature [see Fig. 5(a)]. These results are completely different from those reported on a CeSb single crystal in an applied field of 8.54 T.[25] In the single-crystal sample below T_N, the length change in the 8.54 T field is much smaller than that in zero field (see Fig. 1 in Ref. 25), which is opposite to our results for the 8 T field. This large difference between 8.54 and 8 T results may be due to the presence of a phase boundary near 8 T and 19 K in the *B-T* phase diagram.[12] For the $x=0.15$ alloy an 8 T field reduces the peak height in $\Delta L/L$, but the position of the peak is nearly independent of the field. For CeSb we also investigated the effect of field cooling (FC) on $\Delta L/L$. The CeSb sample was field cooled (in a 8 T field) from 50 to 3 K, and then the field was removed and $\Delta L/L$ was measured (in zero field) with increasing temperature. It was observed that the FC runs shows a large change in length compared with zero-field cooling (ZFC) below 14 K, while above 14 K the FC and ZFC lengths are similar. This may suggest that either the magnetic structure or domain structure and internal stresses is different in the FC state. It would be an interesting to investigate the magnetic structure of CeSb in the FC state using neutron diffraction, which may identify some new magnetic phases in the phase diagram.

The spin-dependent (or 4*f*) contribution to the thermal expansion coefficient, $\alpha_{4f}(T)$, of CeSbNi$_X$ alloys was estimated by subtracting the measured $\alpha(T)$ of LaSbNi$_{0.15}$: $\alpha(\text{LaSbNi}_{0.15}) = \alpha_{\text{ele}}(T) + \alpha_{\text{phon}}(T)$, where the first term is the electronic contribution and the second term is the phonon contribution. For an estimate of $\alpha_{4f}(T)$ for the Ce alloys, we have assumed that the electronic and phonon contributions are the same as in LaSbNi$_{0.15}$, $\alpha_{4f}(T) = \alpha_{\text{mag}}(T) + \alpha_{\text{CF}}(T)$. Here the first term is due to spin-spin correlation in the ordered state as well as in the paramagnetic state and the second term is the contribution arising from the crystalline electric field. It is generally observed that $\alpha_{\text{mag}}(T)$ exhibits a peak, similar to that observed in the heat capacity, at the magnetic ordering temperature.[27] Figure 6 shows $\alpha_{4f}(T)$ as a function of temperature for CeSbNi$_x$ alloys. $\alpha_{4f}(T)$ of CeSb (in zero field) exhibits a sharp peak at 15.4 K, followed by a second broad peak at 12.9 K. The sharp peak in $\alpha_{4f}(T)$ is due to the first-order phase transition from the paramagnetic to antiferroparamagnetic (AFP, $k=2/3, \uparrow\bigcirc\downarrow$; the open circle shows the position of the paramagnetic plane) phase. It is well known that in zero field CeSb exhibits seven magnetic transitions between 17 and 8 K.[11,12,14] However, $\alpha_{4f}(T)$ shows only two well-resolved peaks. A very similar behavior has been observed in the zero-field heat capacity (C_v) of a polycrystalline CeSb sample,[1,28] while seven transitions are observed in the heat capacity of a single crystal of CeSb.[14] The ratio of the heights of the two peaks in the thermal expansion and heat capacity of the polycrystalline samples agrees well. This is expected thermodynamically as $\alpha = \Omega_e \kappa C_v / 3V_m$, where Ω_e is the electronic Grüneisen parameter, κ is the isothermal compressibility, and V_m is the molar volume. From this relation we can estimate Ω_e by scaling $\alpha(T)$ and $C_v(T)$ with the assumption that the value of κ is known and it is temperature independent. We have estimated the value of $\Omega_e = 68$ by scaling $\alpha(T)$ and $C_v(T)$ data near T_N and taking the temperature-independent value of $\kappa = 1$ Mbar^{-1}, a typical value for Ce-based compounds.[29] This value of Ω_e is very high compared with the value of
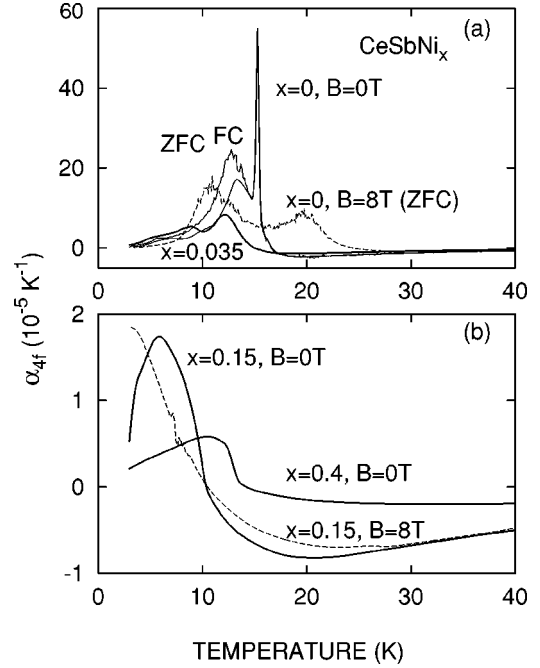

FIG. 6. Thermal expansion coefficient vs temperature for CeSbNi$_X$ ($x=0$, 0.035, 0.15, and 0.4) alloys. The magnetic field was applied parallel to $\Delta L/L$.

1–4 reported for normal metals.[29,30] The high value of $\Omega_e = 10$ was also reported for CePdSb compound, which exhibits its low-dimensional ferromagnetic ordering below 17.5 K.[13]

The $\alpha_{4f}(T)$ measured in an applied field of 8 T exhibits very interesting behavior [Fig. 6(a)]: the sharp peak observed in zero field becomes very broad and moves to a higher temperature (20 K) in the 8 T field. Further, the second peak also broadens in the 8 T field and moves to a lower temperature (11 K). It would be interesting to compare the thermal expansion coefficient results with the heat capacity measured in an applied field of 5 and 10 T.[1,28] In the 5 T field the sharp peak in the $C_v(T)$ has been observed at 22 K due to the para to ferro-para (FP1, with $k=6/11,\uparrow\uparrow\bigcirc\bigcirc\uparrow\uparrow\bigcirc\bigcirc\uparrow\bigcirc$) phase transition. For the 10 T field $C_v(T)$ exhibits a broad peak (second-order type) near 25 K, which is most likely due to FP2 ($k=1/2, \uparrow\uparrow\bigcirc\bigcirc$) to FP' ($k=1/2, \uparrow\uparrow\uparrow\bigcirc$) phase transition, and a sharp peak (first-order type) near 19 K, which is due to FP' ($k=1/2, \uparrow\uparrow\uparrow\bigcirc$) to the ferromagnetic phase ($k=0$). By using the *B-T* phase diagram, we attribute the peak in the $\alpha_{4f}(T)$ at 20 K in the 8 T field to the second-order phase transition from FP3 ($k=4/9, \uparrow\uparrow\uparrow\bigcirc\bigcirc\uparrow\uparrow\bigcirc\bigcirc$) to the boundary of FP' and FP4 ($k=2/5$) phases (see the *B-T* phase diagram in Ref. 5). Further, the *B-T* phase diagram does not show any possibility to assign the peak at 11 K in the 8 T field, which may reveal the existence of new phases in the ferromagnetic region.

The $\alpha_{4f}(T)$ of $x=0.035$ alloy exhibits two broad peaks (of second-order type) at 12.3 and 8.9 K, respectively, with a considerable reduction in absolute value compared to $x=0$ alloy. The position of the first peak agrees with the observed peak at 12.5 K in the dc magnetic susceptibility.[32] We attribute this peak to the paramagnetic to antiferromagnetic phase transition. The second peak in $\alpha_{4f}(T)$ is attributed to the change in the magnetic structure below 9 K as also indicated by the rise in the magnetic susceptibility below 9 K.

This study shows that a Ni composition as low as $x=0.035$ in CeSb is sufficient to suppress the first-order phase transition. The $\alpha_{4f}(T)$ of $x=0.15$ alloy rises sharply below 10.3 K and exhibits a broad peak at 5.8 K. The susceptibility and neutron scattering studies on $x=0.15$ reveal the type-I, $k=(010)$, antiferromagnetic ordering with $T_N=9.5$ K. This shows that the peak (at 5.8 K) in $\alpha_{4f}(T)$ of $x=0.15$ alloy is well below the $T_N=9.5$ K. A very similar behavior has been observed in the ferromagnetic compound CePdSb($T_C=17.5$ K), where the heat capacity and thermal expansion coefficient exhibit a broad peak at 10 K, which is well below $T_C=17.5$ K.[31,33] On the other hand, $\alpha_{4f}(T)$ of $x=0.4$ alloy rises below 13.6 K and exhibits a peak at 11.8 K, which is in agreement with the $T_N=12.5$ K observed through magnetic susceptibility. It is interesting to note that in the paramagnetic state $\alpha_{4f}(T)$ of $x=0$ exhibits a shallow minimum (negative thermal expansion) at 25 K, which becomes weaker with increasing Ni composition and finally disappears for $x=0.4$ composition. A very similar minimum in $\alpha_{4f}(T)$ has been observed in NdCu$_2$, which has been attributed to the effect of the crystalline field on the thermal expansion.[34] Further, the positive sign of $\Delta\alpha(T_N)$ for CeSbNi$_x$ alloys indicates a positive pressure dependence of dT_N/dP, which agrees with the reported value of $+0.7$ K/kbar for CeSb up to $P=2.5$ kbar.[12]

E. Magnetostriction

Figures 7(a)–7(c) show the magnetostriction (MS) isotherms at various temperatures up to the 8 T field ($\mathbf{B}\|\Delta L/L$) for CeSbNi$_x$ ($x=0$, 0.15, and 0.4). Due to the presence of a large hysteresis in CeSb, the magnetostriction isotherms at each temperature were measured after ZFC the sample from 25 K (i.e., above T_N). At 4.8 K, with increasing field MS (or $\Delta L/L$) exhibits a sharp drop, followed by a minimum at 4 T and eventually becomes field independent above 6 T. The decreasing field MS exhibits a minor hysteresis loop between 4 and 8 T and a major hysteresis loop below 4 T. After the first field cycle, the temperature was held fixed (4.8 K) and the field was swept up and down (0 T-8 T-0 T; double-arrows show the direction of field cycle), the crosses in Fig. 7(a) represent the change of the MS during this cycle. The third cycle of the field gave the same results as that of the second cycle. The above behaviors were reproduced when the sample was heated up to 25 K and ZFC to 4.8 K. This shows that the hysteresis is an intrinsic property of the sample. It is interesting to note that, after the field cycles, the zero-field length can be recovered by heating the sample above T_N and ZFC. The sharp decrease in the MS below 4 T is due to an abrupt change in the magnetic structure at an applied field of 3.7 T as seen through magnetization measurements.[23] At 15 K a very small hysteresis was observed in the MS, while no hysteresis was observed at 20 K and above it. At 25 and 30 K, the MS exhibits a B^2 dependence up to 8 T, while a small deviation from B^2-dependent behavior is observed at 20 K. The latter may suggest the presence of spin-spin correlation just above T_N. The magnitude of the MS of CeSb even in the paramagnetic state is very large compared to that observed in Ce-based heavy fermion compounds, such as CeCu$_2$ and CeCu$_2$Si$_2$.[35] The observed B^2 dependence of MS in the paramagnetic state is in
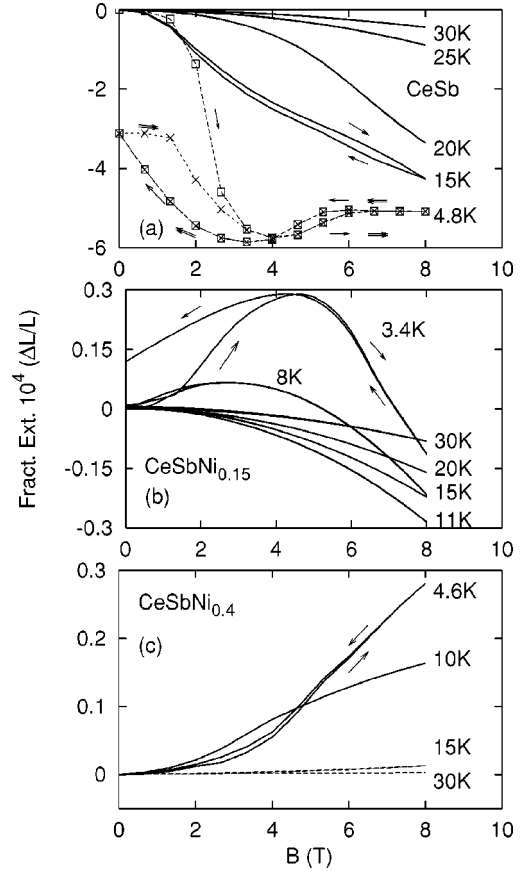

FIG. 7. The normalized magnetostriction vs applied field field ($\mathbf{B}\|\Delta L/L$) for CeSbNi$_X$ ($x=0$, 0.15, and 0.4) alloys at various temperatures. The arrows show the direction of the field cycle. For $x=0$, squares represent the first cycle of the field sweep (direction shown by single arrows) after ZFC from 25 K and crosses represents the second cycle of the field sweep (direction shown by double arrows), immediately after the first cycle.

agreement with the prediction of the Maxwell relation $[\partial\lambda_i/\partial B]_{\sigma_i}=-[\partial M/\partial\sigma_i]_B$, with M the magnetic moment per unit volume, λ_i the magnetostrictive strain, and σ_i the stress corresponding to λ_i.[36]

The magnetostriction of $x=0.15$ at 3.4 K exhibits a peak at 4.5 T and a small hysteresis compared with $x=0$. The peak in the MS is attributed to a metamagnetic transition as observed in the magnetization measurements at 6.5 T at 1.5 K.[15] With increasing temperature the peak and hysteresis decrease and MS exhibits a maximum negative value at 11 K. The absolute value of the MS decreases with further increasing temperature. Between 11 and 30 K the MS exhibits B^2-dependent behavior. A similar behavior of the MS was observed for $\mathbf{B}\perp\Delta L/L$ direction (data not shown here), except the peak position was at 6.5 T at 3.3 K with smaller hysteresis and the zero-field length was the same before and the after the field cycle. On the other hand, the MS of $x=0.4$ below T_N is positive (i.e., the length increases with the field) with very little hysteretic behavior, while negligible positive MS was observed above T_N. It would be interesting to compare the present MS results with that of Ce$_{1-x}$La$_x$Sb ($x=0.2$, 0.3, and 0.5) alloys.[25] At 4.2 K, Ce$_{0.8}$La$_{0.2}$Sb exhibits MS of 4.8×10^{-4} at the 8 T field, while almost negligible positive MS was observed for Ce$_{0.5}$La$_{0.5}$Sb up to the 8 T field
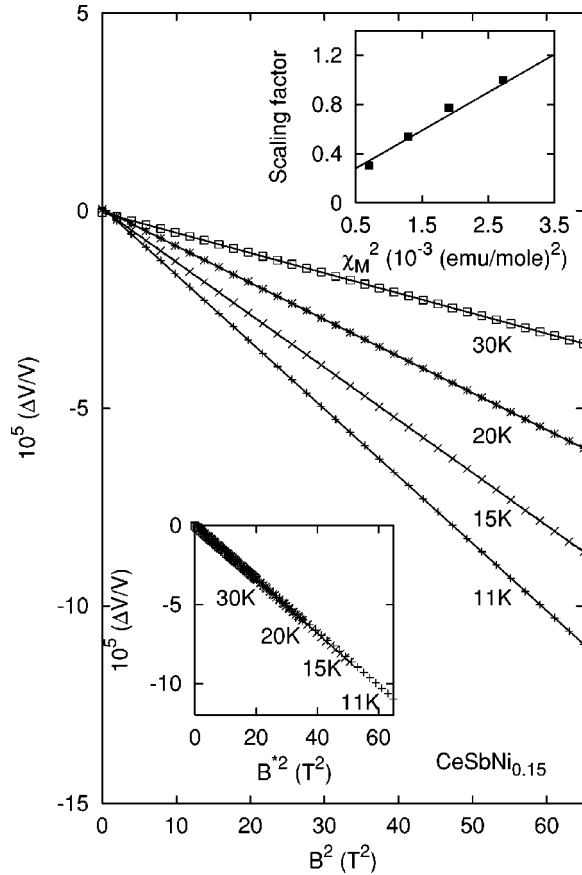
FIG. 8. The volume magnetostriction (VMS) vs B^2 for CeSbNi$_{0.15}$ at various temperatures in the paramagnetic state. The bottom inset shows the scaling of VMS of 15, 20, and 30 K data to that of 11 K data using a temperature-dependent scaling factor (SF). Here the effective field $\mathbf{B}^*(T) = \mathbf{B}(T) \times \mathrm{SF}(T)^{1/2}$. The top inset shows the scaling factor vs χ^2 at 11, 15, 20, and 30 K. The solid line represents a linear behavior.

at 4.2 K. These results show that the large MS and the discontinuous change in the length (in zero field) at T_N observed in CeSb disappears with either incorporation of Ni at an interstitial site or substitution of Ce by La. The implication is that the electronic density or chemical pressure is more important than the coherent Ce lattice for large magnetostriction as well as a thermal expansion anomaly near T_N.

For $x=0.15$ alloy we have calculated the volume magnetostriction (VMS) at various temperatures in the paramagnetic state as $\Delta V/V = (\Delta L/L)\| + 2(\Delta L/L)\perp$, where in the first term the field was applied parallel to $\Delta L/L$ and in the second term it was perpendicular to $\Delta L/L$. The VMS also exhibits B^2 dependence in the paramagnetic state (Fig. 8). The VMS of $x=0.15$ alloy is very high and negative compared with small positive VMS observed in many Ce-based compounds.[35] A negative VMS has been observed for Yb-based compounds.[35] In the paramagnetic state VMS can be expressed as $\Delta V/V = C\kappa\chi^2 B^2$, where C is the magnetovolume coupling constant, κ is the isothermal compressibility, and χ is the paramagnetic susceptibility. This relation shows that by using a temperature-dependent scaling factor it is possible to obtain a unique scaling curve of VMS for all temperatures. We have scaled the VMS data of 15, 20, and 30 K to that of 11 K, which exhibits good scaling behavior

(bottom inset to Fig. 8). The temperature dependence of the scaling factor exhibits almost similar behavior to that of $\chi^2(T)$ (top inset to Fig. 8). This indicates that the product of $C\kappa$ is temperature independent for $x=0.15$. From the slope of scaling factor versus χ^2 and $\Delta V/V$ versus B^{*2} curves (insets to Fig. 8), we have estimated the value of the product of $C\kappa = -5.3(\pm 0.6) \times 10^{-4}(\mu_B^{-2})$.

IV. CONCLUSIONS

Inelastic neutron scattering studies of CeSbNi$_X$ ($x=0.08$ and 0.15) show a well-defined crystal field excitation at 4.06 and 5.02 meV, respectively, and the quasielastic response centered at zero energy. The temperature dependence of the intensity of the quasielastic and inelastic lines reveals that the crystal field ground state is a doublet Γ_7 in CeSbNi$_{0.15}$. The increase in the crystal field splitting with x and the isotropic magnetic properties of CeSbNi$_{0.15}$ compared with the parent compound CeSb indicate that the *p-f* mixing has reduced considerably with the Ni incorporation in CeSb. The strong *p-f*(Γ_8) mixing pushes the Γ_8 down close to the Γ_7 level and hence gives a small CF splitting in CeSb (Ref. 7–10) compared with the value of 22.75 meV expected from the point charge model and using the values of other members of the rare-earth compounds in this series.[6] The collapse of the *p-f* mixing in CeSbNi$_x$ could arise through an overlap between the *p* band of Sb and the *d* band of Ni, which fills the *p* holes that mix strongly with the Γ_8 state of Ce^{3+}. The reduction in the anisotropic magnetic exchange, as observed in the present study, has been also reported in R_{1-x}Ce$_x$Sb ($R=$La and Y), but the crystal field splitting remains almost unchanged.[4,37] An elastic neutron scattering study of CeSbNi$_{0.15}$ shows the simple type-I antiferromagnetic structure with wave vector $k=(010)$. The temperature-dependent susceptibility of CeSbNi$_{0.15}$ has been analyzed on the basis of the crystal field model and using the crystal field parameter obtained from the inelastic neutron scattering study.

The thermal expansion exhibits a dramatic change in behavior with Ni composition. The thermal expansion coefficient exhibits a first-order transition at T_N in CeSb, which disappears with incorporation of Ni composition as low as $x=0.035$. The first-order transition was not observed in the thermal expansion coefficient measured in an applied field of 8 T. The thermal expansion coefficient of $x=0.15$ (in zero field) exhibits a peak at 5.8 K, which is well below the $T_N = 9.5$ K. The estimated value of the electronic Grüneisen parameter of CeSb is very high compared with the value of normal metal and other Ce-based compounds.[29,30] CeSb exhibits a large magnetrostriction in the ordered state as well as in the paramagnetic state. In the paramagnetic state $x=0$, 0.15, and 0.4 alloys exhibit a B^2 dependence of MS, which agrees with the prediction of the Maxwell relation. The absolute value of the MS is reduced considerably in the Ni-incorporated alloys, which reflects a large reduction in the magnetovolume coupling constant for these alloys. The MS of $x=0.15$ in the paramagnetic state exhibits a scaling law from which we have estimated the product of the magnetovolume coupling constant and the isothermal compressibility.

Beside the effect of the p-f mixing on the CF splitting in $CeSbNi_x$ alloys, there would be some contribution to the crystal field from the Ni atoms. The Ni atoms occupy interstitial sites in CeSb; hence, the change in the physical properties of Ce ions in $CeSbNi_x$ alloys is also expected due to a local (structural and charge) distortion on the Ce neighbors due to the random distribution of Ni atoms. This would lift the degeneracy of the excited crystal field level (Γ_8) and increase the linewidth of the crystal field excitations and the magnetic transition. If the local structural distortion was significant, one would expect two CF excitations in $CeSbNi_x$ alloys as observed in the cubic $CePd_3Si_x$ ($x=0.07-0.15$)

(Ref. 38): Si atoms also occupy interstitial sites in the cubic structure of $CePd_3$. The absence of two crystal field excitations in $CeSbNi_x$ suggests that the local structural distortion is not very significant. On the other hand, the increase in the linewidth of the CF excitation with x reflects the presence of the charge disorder.

ACKNOWLEDGMENTS

[1] See, for example, T. Suzuki, Jpn. J. Appl. Phys., Part 1 **8**, 267 (1993).

[2] B. D. Rainford, K. C. Turberfield, G. Busch, and O. Vogt, J. Phys. C **1**, 679 (1968).

[3] H. Heer, A. Furrer, W. Hälg, and O. Vogt, J. Phys. C **12**, 5207 (1979).

[4] B. Hälg, A. Furrer, and O. Vogt, J. Magn. Magn. Mater. **54–57**, 705 (1986).

[5] D. Davidov, E. Bucher, L. W. Rupp, Jr., L. D. Longinotti, and C. Rettori, Phys. Rev. B **9**, 2879 (1974).

[6] R. J. Birgeneau, E. Bucher, J. P. Maita, L. Passell, and K. C. Turberfield, Phys. Rev. B **8**, 5345 (1973).

[7] B. R. Cooper, J. Magn. Magn. Mater. **29**, 230 (1982).

[8] H. Takahashi and T. Kasuya, J. Phys. C **18**, 2695 (1985).

[9] T. Kasuya, in *Theory of Heavy Fermion and Valence Fluctuations*, edited by T. Kasuya and T. Saso (Springer, Berlin, 1985), p. 2.

[10] H. Takahashi, K. Takegahara, Yanase, and T. Kasuya, in *Valence Instabilities*, edited by P. Watcher and H. Boppart (North-Holland, Amsterdam, 1982), p. 379.

[11] J. Rossat-Mignod, P. Burlet, J. Villain, H. Bartholin, W. Tscheng-Si, and D. Florence, Phys. Rev. B **16**, 440 (1977).

[12] T. Chattopadhyay, P. Burlet, J. Rossat-Mignod, H. Bartholin, C. Vettier, and O. Vogt, Phys. Rev. B **49**, 15 096 (1994).

[13] F. Hulliger, M. Landolt, H. R. Ott, and R. Schmelczer, J. Low Temp. Phys. **20**, 269 (1975).

[14] J. Rossat-Mignod, P. Burlet, H. Bartholing, O. Vogt, and R. Lagnier, J. Phys. C **13**, 6381 (1980).

[15] D. T. Adroja, M. H. Jung, Y. Shibata, and T. Takabatake, J. Phys.: Condens. Matter **11**, 3687 (1999).

[16] T. Chatterji, D. T. Adroja, M. H. Jung, T. Takabatake, and P. C. Riedi (unpublished).

[17] S. W. Lovesy, *Theory of Neutron Scattering for Condensed Matter* (Oxford University Press, Oxford, 1984), Vols. 1 and 2.

[18] K. W. H. Stevens, Proc. R. Soc. London, Ser. A **65**, 209 (1952); M. T. Hutchings, Solid State Phys. **16**, 227 (1964).

[19] K. R. Lea, M. J. M. Leask, and W. P. Wolf, J. Phys. Chem. Solids **23**, 1381 (1962).

[20] P. G. de Gennes, in *Magnetism*, edited by G. T. Rado and H. Suhl (Academic, New York, 1963), Vol. 3, p. 115.

[21] J. Rossat-Mignod, P. Burlet, S. Quezel, J. M. Effantian, D. Delacôte, H. Bratholin, O. Vogt, and D. Ravot, J. Magn. Magn. Mater. **31–34**, 398 (1983).

[22] N. Shibata, C. Ishii, and K. Ueda, Phys. Rev. B **52**, 10232 (1995).

[23] G. Busch and O. Vogt, Phys. Lett. **25A**, 449 (1967).

[24] A. Furrer, W. Bührer, H. Heer, W. Hälg, J. Beneš, and O. Vogt, *Neutron Inelastic Scattering, Proceedings, Grenoble, 1972* (International Atomic Energy Agency, Vienna, 1972), p. 563.

[25] M. Sera, T. Fujita, T. Suzuki, and T. Kasuya, in *Valence Instabilities*, edited by P. Wachter and H. Boppart (North-Holland, Amsterdam, 1982), p. 435.

[26] D. F. McMorrow, J. G. Lussier, B. Lebech, S. Aa Sørensen, M. J. Christensen, and O. Vogt, J. Phys.: Condens. Matter **9**, 1133 (1997).

[27] M. J. Thornton, J. G. M. Armitage, G. J. Tomka, P. C. Riedi, R. H. Mitchell, M. H. Houshiar, D. T. Adroja, B. D. Rainford, and D. Fort, J. Phys.: Condens. Matter **10**, 9485 (1998).

[28] T. Kasuya, Y. S. Kwon, T. Suzuki, K. Nakanishi, F. Ishiyam, and K. Takegahara, J. Magn. Magn. Mater. **90&91**, 389 (1990).

[29] J. D. Thompson and J. M. Lawrence, in *Lanthanides/Actinides: Physics-II*, Vol. 19 of *Handbook on the Physics and Chemistry of Rare Earths*, edited by K. A. Gschneidner, Jr., L. Eyring, G. H. Lander, and G. R. Choppin (Elsevier, New York, 1994), p. 383.

[30] M. J. Thorton, Ph.D. thesis, St. Andrews University, 1996: the estimated value of the electronic Grüneisen paramater for the nonmagnetic metallic compound LaAgGe is 1.3 in this reference.

[31] M. J. Thorton, J. G. M. Armitage, R. H. Mitchell, P. C. Riedi, D. T. Adroja, B. D. Rainford, and D. Fort, Phys. Rev. B **54**, 1 (1996).

[32] M. H. Jung, D. T. Adroja, F. Iga, T. Suzuki, T. Fujita, and T. Takabatake, Physica B **281–282**, 443 (2000); M. H. Jung, D. T. Adroja, T. Takabatake, I. Oguro, S. Kawasaki, and K. Kindo (unpublished).

[33] O. Trovarelli, J. G. Sereni, G. Schmerber, and J. P. Kappler, Phys. Rev. B **49**, 15 179 (1994).

[34] E. Gratz, M. Loewenhaupt, M. Divis, W. Steiner, E. Bauer, N. Pillmayr, H. Müller, H. Nowothy, and B. Frick, J. Phys.: Condens. Matter **3**, 9297 (1991).

[35] J. Zieglowski, H. U. Häfner, and D. Wohlleben, Phys. Rev. Lett. **56**, 193 (1986).

[36] K. N. R. Taylor and M. I. Darby, *Physics of Rare Earth Solids* (Chapman and Hall, London, 1972), p. 146.

[37] B. R. Cooper and O. Vogt, J. Phys. (Paris), Colloq. Suppl. No. 2–3, C1-1026 (1971).

[38] B. D. Rainford, D. T. Adroja, and S. J. Dakin (unpublished).